Int J Clin Exp Med 2016;9(5):7818-7827
www.ijcem.com /ISSN:1940-5901/IJCEM0020259

Original Article

Astragaloside IV stimulates angiogenesis after myocardial infarction by regulating microRNA-21 expression

Peng Yu[1,2*], Songyi Cheng[1*], Li Yang[1], Yu Zhang[3], Jiandong Chen[2], Xiaohu Chen[2]

[1]First Clinical Medical College, Nanjing University of Chinese Medicine, Nanjing 210023, P. R. China; [2]Department of Cardiology, Jiangsu Province Hospital of Traditional Chinese Medicine, The Affiliated Hospital of Nanjing University of Chinese Medicine, Nanjing 210029, P. R. China; [3]School of Pharmacy, Nanjing University of Chinese Medicine, Nanjing 210023, P. R. China. [*]Equal contributors.

Received November 22, 2015; Accepted March 25, 2016; Epub May 15, 2016; Published May 30, 2016

Abstract: Astragaloside IV (AS-IV) was regarded as the main effective ingredient of Astragalus membranaceus, a kind of traditional Chinese herbal medicine, which was widely used in clinical practice, especially in treating cardiovascular diseases. In this work acute myocardial infarction (AMI) rat model was established by permanent ligation of the left anterior descending (LAD) coronary artery, and then the AMI rats were randomly treated with AS-IV or vehicle. We observed that after AS-IV treatment pathological changes was improved in infarcted tissue and microvascular density around infarcted site was increased compared with control, moreover, AS-IV could up-regulate mRNA and protein expression of VEGF, p-AKT together with miR-21 expression in tissue around infarcted site. Further study on EA-hy926 cells indicated that both AS-IV and miR-21 mimic could promote angiogenesis in vitro. Research also revealed that AS-IV regulated VEGF synthesis by regulating miR-21, and the angiogenic effects of AS-IV could be reversed by miR-21 inhibitor, which significantly reduced the proliferation, migration, and tube-forming capacity of EA-hy926 cells. Collectively our results demonstrate that AS-IV was a novel regulator of VEGF signaling pathway and angiogenesis through regulating miR-21 in vivo and vitro.

Keywords: Astragaloside IV, angiogenesis, miR-21, myocardial infarction

Introduction

Astragaloside IV (AS-IV, 3-O-β-D-xylopyranosyl-6-O-β-D-glucopyranosylcycloastragenol), the main effective components purified from the Chinese medical herb Astragalus membranaceus (Fisch) Bge, has long been widely used for the treatment of various diseases including different systems [1-4]. AS-IV also have been developed as a novel cardio-protective agent [5], researchers have dedicated long period on the clinical and experimental study on its effectiveness and mechanisms in treating cardiovascular diseases from different aspects, and have assured its important pharmacological effects on protecting cardiovascular system, including a protection against arrhythmias [6], ischemia and reperfusion injury [7], oxidation injury [8], cardiac hypertrophy [9] and myocarditis [10]. Recently, some studies [11, 12] including ours [13, 14] have suggested that AS-IV also has the ability to promote angiogenesis via several pathways in vitro, moreover, AS-IV enhances healing and anti-scar effects on wound repair by promoting angiogenesis in rat [15, 16]. Meanwhile, angiogenesis therapy is consistently being profoundly investigated as a novel non-invasive approach for ischemic heart disease [17]. All those findings above hint at the potential for the application of AS-IV as a pro-angiogenesis therapeutic agent in the management of myocardial ischemia. However, the central mechanism of AS-IV in regulating angiogenesis remains to be elucidated.

MicroRNAs (miRNAs) are endogenous small non-coding ribonucleotides that regulate expression of target genes governing diverse biological functions, briefly, mature miRNA incorporates into the RNA-induced silencing complex

(RISC), which directs the miRNA to the target mRNA leading either to translational repression or degradation of the target mRNA [18]. During the last few years, a plethora of work has been published characterizing cell specific effects of miRNA-21 (miR-21), not only in myocytes, endothelial cells, inflammatory cells [19-21], but also in cardiac fibroblasts physiologically and pathologically with cardiac stress [22, 23] leading to profound effects on the cardiac function. It is also reported that miR-21 played a necessary role in regulation of both cardiac valvulogenesis and angiogenic phenotype of microvascular endothelial cells [24, 25], suggesting that regulating miR-21 maybe a target of treating ischemic heart disease by promoting angiogenesis.

AS-IV was demonstrated to be a potential therapeutic agent for treating viral myocarditis, research showed that AS-IV exerts antiviral effects against CVB3 by upregulating expression of IFN-gamma mRNA [10]. This study indicated that mRNA may be a target on AS-IV's protection. Given that mRNA expression can be regulated by miRNA, whether AS-IV had an effect on miRNA drew our interest and it was totally not been studied. In this research, we intend to elucidate whether AS-IV promotes angiogenesis by regulating miR-21 expression and the potential mechanism of miR-21-mediated angiogenesis.

Materials and methods

Rat model of AMI

Sprague-Dawley male rats (age, 10 weeks; weight, 250±20 g) purchased from the Animal Center of Nanjing Medical University were employed in this study. The study complied with Guide for the Care and Use of Laboratory Animals of the National Institutes of Health and standards for the Care and Use of Laboratory Animals (Laboratory Animal Center of Nanjing University of Chinese Medicine). The animal protocol was approved by the Ethics Review of Lab Animal Use Application of Nanjing University of Chinese Medicine.

Briefly, Intraperitoneal Injection of pentobarbital sodium (50 mg/kg) was performed before surgery. After fixed on the pad and linked to electrocardiograph, endotracheal intubation was carried out on the rat; a ventilator was used to maintain respiration. Carefully dissected pectoralis major and serratus anterior, the heart was then exposed between ribs. LAD was ligated with a 6-0 polypropylene suture approximately midway between left atrium and pulmonary conus of the heart. In the sham group, operations were carried out by the same method but without tying the suture on the LAD. ST segment elevated on electrocardiograph was a sign of successful modeling, pale color of left ventricle anterior and apex part also could be seen in successful AMI model. Sucked out excess air in the thorax with a syringe, then quickly closed thoracic cavity with standard produces.

Grouping and drug administration

Operated rats survived for 12 h were randomly divided into groups below: AMI model group (n=8), AS-IV low-dose group (n=8) and AS-IV high-dose group (n=8). In addition, 8 sham-operation rats served as sham group. AS-IV was purchased from the National Institute for the Control of the Pharmaceutical and Biological Products (Beijing, China) and its purity was greater than 98%. The rats in low-dose group and high-dose group received continually intragastric administration with AS-IV one day after surgery, 30 mg/kg/d and 100 mg/kg/d, respectively; rats in model group and sham group were intragastric administrated with equivalent distilled water. Rats were sacrificed at 14th day.

Histopathology

To evaluate the morphological changes, the hearts were harvested, washed in PBS and fixed in 4% paraformaldehyde for overnight and embedded in paraffin. Each heart was cut into sections of 4 μm sections and stained with hematoxylin and eosinstaining. And each section was imaged by a microscopy (Nikon, Japan).

Immunohistochemistry staining

In order to evaluate microvascular and arteriole formation, CD34+ and α-SMA immunohistochemistry (IHC) staining were employed. Fixed tissues were cut into 4 μm sections and were incubated with anti-CD34 antibody and anti-α-SMA antibody (Abcam, Cambridge, UK) at 4°C overnight, followed by sequential incubations of biotinylated (Vector) secondary antibody for 20

minutes at room temperature. Then sections were color-developed by DAB and sequentially counterstained with hematoxylin. The positive signals of CD34 and α-SMA were stained with orange-yellow. Percentage of angiogenesis was count in area that bearing positive CD34 and α-SMA signals was analyzed under microscope.

Cell culture

Vitro studies were also employed to figure out deeper mechanism of AS-IV's proangiogenic ability. EA-hy926 cells (ATCC, Manassas, VA, USA) were cultured in DMEM (Gibco, USA) supplemented with 10% fetal bovine serum (Gibco, USA), 100 U/ml penicillin (Hycloue, Thermo scientific, USA) and 100 μg/ml streptomycin (Hycloue, Thermo scientific, USA). AS-IV was purchased as mentioned above, and it was dissolved in dimethyl sulfoxide (DMSO), the final DMSO concentration was less than 0.1%. The EA-hy926 cells were cultured in humidified air with 5% CO_2 at 37°C. The whole experimental process conformed to the principles outlined in the Declaration of Helsinki. All participants gave written informed consents and the study was approved by the ethics committee of Jiangsu Provincial Hospital of TCM.

Cell proliferation assay

Viability of cells was assessed by Cell Counting Kit-8 (CCK-8) assay (Dojindo Laboratories, Kumamoto, Japan). In brief, cells were seeded in each well of a 96-well plate according to the density of 2×10^4 cells for each well after transfected with the indicated miRNA, 24 h later, cells were exposed to 100 μg/L AS-IV. Premixed CCK-8 and medium (10 μL) were added into 96-well plates, and cells were then incubated for 0.5-1 h at 37°C. The values of A450 were obtained with the 3,550 automatic detectors from Beckman (Brea, CA).

Tube formation

A Matrigel tube-formation assay was also performed to assess in vitro angiogenesis. Growth factor-reduced Matrigel (BD) was placed in 96-well culture plates and allowed to set at 37°C for 1 h. Then 1×10^4 EA-hy926 cells were added to each well and incubated in basic medium. Five fields were counted for each well. The length of the tube was measured by Image-Pro Plus 6.0 (Media Cybernetics, Bethesda, MD).

Cell transfection and infection

The miR-21 mimics and inhibitors were purchased from RiBoBio (Guangzhou, China). Transfection of miRNAs was performed by using Lipofectamine 2000 (Invitrogen, CA, USA) according to the protocol. The final concentration of miRNA mimics and miRNA inhibitors were 50 nM and 100 nM, respectively.

Quantitative real-time PCR

The total RNA was isolated using Trizol-reagent (Invitrogen Company) according to manufacturer's instructions. Real-time PCR was used to measure the expression of VEGF, AKT and miR-21 in myocardial tissue and EA-hy926 cells. Real-time PCR was performed with the following PCR primers: GAPDH: forward 5'-CGGGAAACTGTGGCGTGAT-3' and reverse 5'-CAAAGGTGGAGGAGTGGGT-3'; U6: forward 5'-CTCGCTTCGGCAGCACA-3' and reverse 5'-AACGCTTCACGAATTTGCGT-3'; VEGF: forward 5'-ATGAACTTTCTGCTGTCTTG-3' and reverse 5'-TGCATGGTGATGTTGGAC-3'; AKT: forward 5'-GAGGAGCGGGAAGAGTG-3' and reverse 5'-GAGACAGGTGGAAGAAGAGC-3'. miR-21: forward 5'-GCGCGCTAGCTTATCAAGCTGATG-3' and reverse 5'-GTGCAGGCTCCGAGGT-3'. SYBR-Green Universal Master Mix kit (ABI) was employed to detect the levels of these genes. The program was initially run for 12 min at 95°C, followed by 40 cycles of 10 sec at 95°C, 25 sec at 60°C and 25 sec at 72°C. MiR-21 expression levels were normalized to the U6 rRNA endogenous control, while other RNA was normalized to GAPDH. Fold changes were calculated using the ΔΔCt method.

Western blotting

Total protein in vivo was obtained from left ventricular myocardial tissues. EA-hy926 cells were lysed in Lysis Buffer containing protease inhibitor and phosphatase inhibitor. After centrifugation, they were followed by sonication and heat denaturation. A total of 20 μg protein lysates were electrophoresed and separated on 6%-12% SDS-PAGE and transferred onto nitrocellulose membranes (Invitrogen Company, USA). After blocking in 1× TBST, 5% nonfat dry milk, 0.2% Tween-20 at room temperature for 30 min, the membranes were incubated with the primary antibodies in blocking buffer (1× TBST, 3% nonfat dry milk, 0.2% Tween-20) overnight at 4°C. The membranes were washed

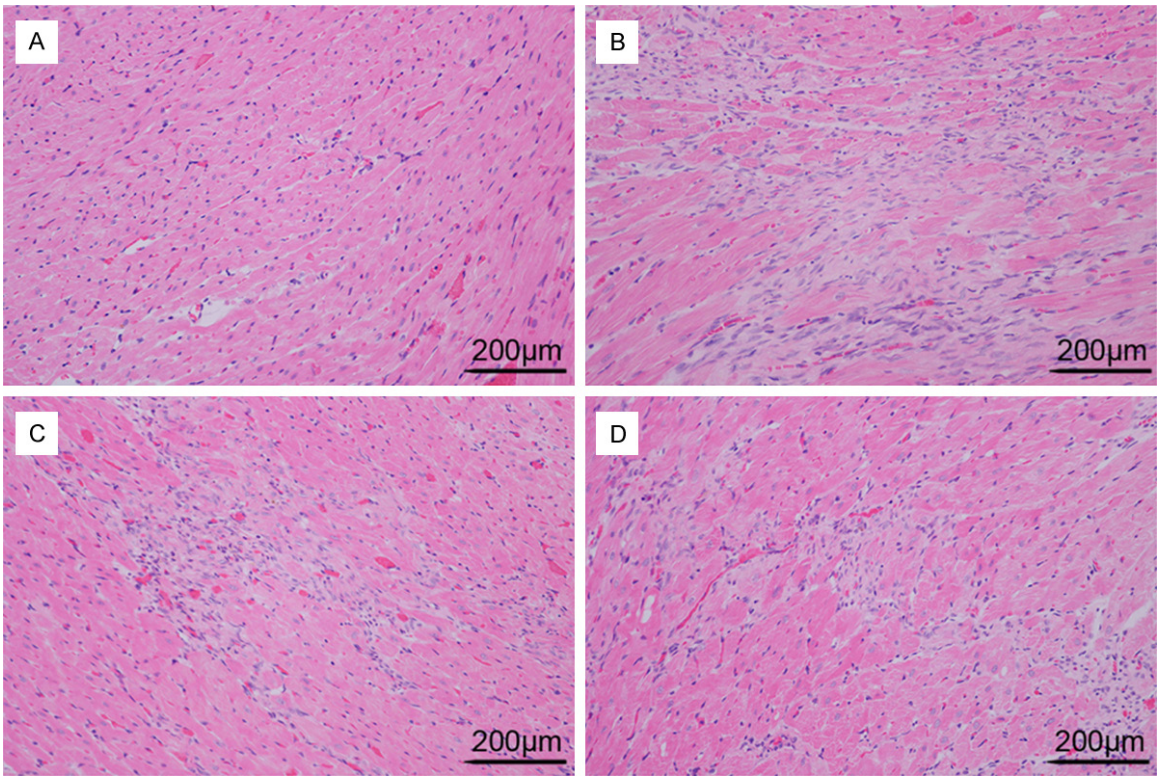

Figure 1. A. Shamgroup; B. Modelgroup; C. AS-IV 30 mg/kg/d group; D. AS-IV 30 mg/kg/d group. H-E. Staining demonstrated the intense inflammatory response and myocardial cells arranged irregularly after AMI in model group compared to sham group, and it was alleviated in AS-IV treating group in a dose-dependent manner.

three times for 30 min with 1× TBST and then incubated with secondary antibodies. After final washes with 1× TBS, 0.2% Tween-20, the signals were detected using ECL chemiluminescence reagents (Pierce). Antibodies of VEGF (1:200, Santa Cruz, USA), p-AKT (1:800, Cell Signaling Technologies, USA) and β-actin (1:1000, Santa Cruz, USA) were used in this assay.

Statistical analysis

Results were expressed as the mean ± standard error of the mean (SEM). Statistical analysis was performed by a one-way analysis of variance (ANOVA) followed by a Student-Newman-Keul'stest (SNK) with SPSS 22.0 software (IBM, Armonk, NY, USA). Difference was considered significant at $P<0.05$.

Results

AS-IV treatment improved pathological changes in infarcted tissue

After 2 weeks treatment, as shown by H-E staining, in the untreated group (**Figure 1B**), the surviving myocardial cells were found in the border zones and arranged irregularly, and there were much infiltration of inflammatory cells. However, in AS-IV treatment group (**Figure 1C** and **1D**), most of myocardial cells were normal and arranged in an orderly manner, and the area of necrosis was smaller compared to the untreated group.

AS-IV treatment promoted angiogenesis after AMI

Compared with AMI model group, microvascular and arteriole density around infarcted site in AS-IV treatment groups was enhanced significantly in a dose-dependent manner (**Figure 2A-D** and **2F-I**). protein and the total RNA was extracted from myocardial tissue, Western blot and real-time PCR was used to detect the VEGF, VEGF mRNA, p-AKT, AKT mRNA and miR-21 level (**Figure 3**). Protein expression of VEGF and p-AKT in groups with AS-IV treatment was also upregulated compared to untreated groups; AS-IV was also capable of enhancing level of mRNA of VEGF and AKT, together with miR-21 in the area around infarcted site.

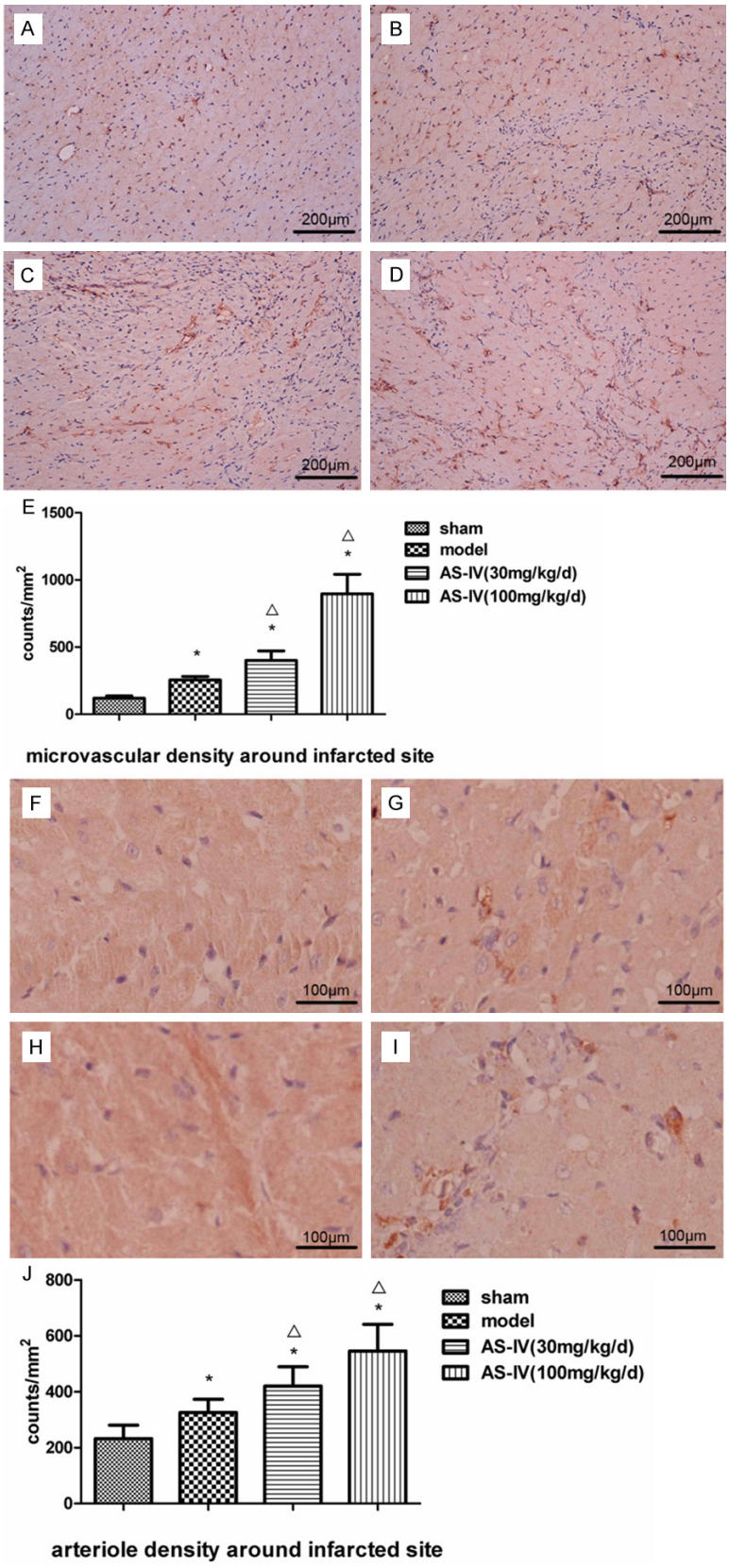

Figure 2. (A and F) Sham group; (B and G) Model group; (C and H) AS-IV 30 mg/kg/d group; (D and I) AS-IV 30 mg/kg/d group. (A-D) CD34+ and (F-I) α-SMA Immunohistochemistry staining represent newly formed microvascular and arteriole in different groups, respectively (n=8 per group). Figures showed the angiogenic potential of AS-IV treatment after AMI in rats. (E & J) Microvascular density and arteriole density were calculated in each group. *: P<0.05 versus sham group, △: P<0.05 versus model group.

AS-IV stimulated cell proliferation, VEGF expression and miR-21 expression

In vitro study, AS-IV significantly stimulated EA-hy926 cells proliferation at the concentration of 10 to 150 μg/mL, whereas 100 μg/mL AS-IV demonstrated the most significant effect (**Figure 4A**). In addition, we applied real-time PCR and Western blot to detect the miR-21 expression and VEGF expression when the cells were treated with AS-IV (0, 10 μg/mL, 30 μg/mL, 100 μg/mL) for 24 h (**Figure 4B-D**), whereas AS-IV at 100 μg/mL notably stimulated miR-21 expression and VEGF expression significantly, compared with the control group.

Transient transfection of miR-21 mimic enhanced tube formation ability of EA-hy926 cells compared with AS-IV

Cells were treated with the miR-21 mimics and inhibitors for 48 h, another group with 100 μg/mL AS-IV for 24 h. Then capillary-like structures were examined further (**Figure 5**). Treatment with AS-IV and miR-21 mimic promoted cell tube formation and transient transfection of miR-21 mimic showed a significant effect compared with AS-IV group. However, the effect of AS-IV was abrogated by miR-21 inhibitor. These results together indicate that miR-21

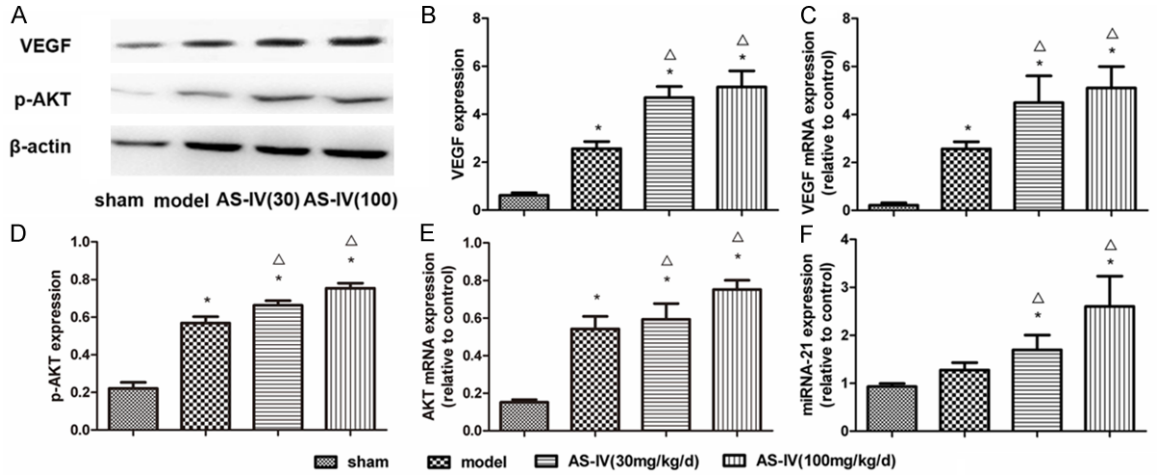

Figure 3. A. Cellularlysate from myocardial tissue was used to measure VEGF and p-AKT levels by western blot. B. Bar graph represents VEGF levels. C. Total RNA was extracted from myocardial tissue, real-time PCR was used to detect the VEGF mRNA levels. D. Bar graph represent p-AKT levels. E. Total RNA was extracted from myocardial tissue, real-time PCR was used to detect the AKT mRNA levels. F. MiR-21 expression in each group. Data are expressed as the mean ± S.E.M. Data shown are representative of three independent experiments. *: P<0.05 versus sham group, △: P<0.05 versus model group.

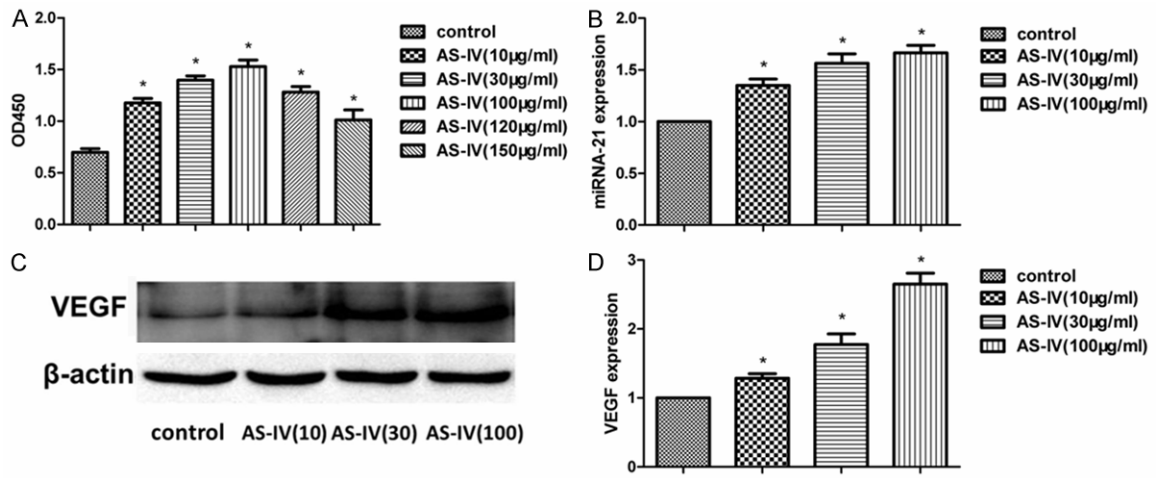

Figure 4. A. The effects of AS-IV on cell proliferation were determined by CCK-8 assay after treat with AS-IV (10, 30, 100, 120, 150 μg/mL); B. Effects of AS-IV on the level of miR-21 expression. Cells were treated with AS-IV (0, 10 μg/mL, 30 μg/mL, 100 μg/mL) for 24 h. Then, the total RNA was extracted, and real-time PCR was used to detect the miR-21 level. C. Cells were treated with AS-IV (10, 30, 100 μg/mL); Cellular lysate from EA-hy926 cells was collected to measure VEGF levels by western blot. D. Bar graph represents VEGF levels. Data are expressed as the mean ± S.E.M. Data shown are representative of three independent experiments. *: P<0.05 versus control group.

mimic can activate angiogenesis like AS-IV. Based on these results, we hypothesize that miR-21 may be involved in the process of cell proliferation and angiogenesis by AS-IV in EA-hy926 cells, and miR-21 maybe regulates angiogenesis in EA-hy926 cells.

Effects of AS-IV on the level of VEGF, AKT mRNA and VEGF, AKT protein expression

Total RNA and protein were extracted. The real-time PCR and western blotting were performed to detect the VEGF, AKT mRNA level and protein levels of VEGF as well as the p-AKT expression. It was shown that the VEGF mRNA level increased nearly 1.5-fold in AS-IV group compared with the normal group, and nearly 2-fold in miR-21 mimic group compared with the normal control group; treatment with AS-IV raised AKT mRNA expression over 1.5-fold compared with the control, and nearly 2-fold in miR-21 mimic group compared with the normal control group. The effect of AS-IV increasing VEGF

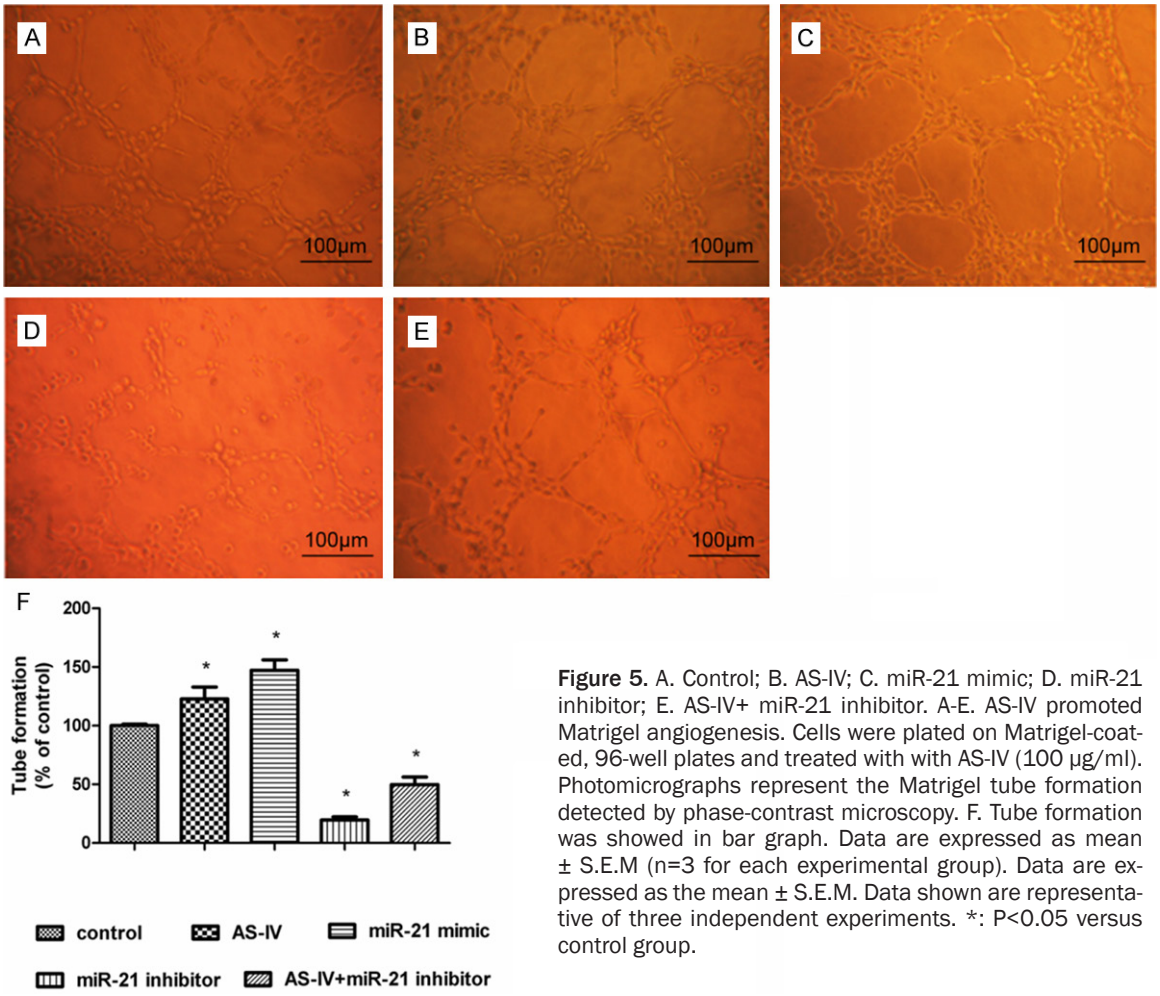

Figure 5. A. Control; B. AS-IV; C. miR-21 mimic; D. miR-21 inhibitor; E. AS-IV+ miR-21 inhibitor. A-E. AS-IV promoted Matrigel angiogenesis. Cells were plated on Matrigel-coated, 96-well plates and treated with with AS-IV (100 μg/ml). Photomicrographs represent the Matrigel tube formation detected by phase-contrast microscopy. F. Tube formation was showed in bar graph. Data are expressed as mean ± S.E.M (n=3 for each experimental group). Data are expressed as the mean ± S.E.M. Data shown are representative of three independent experiments. *: P<0.05 versus control group.

mRNA and AKT mRNA was abrogated by miR-21 inhibitor (**Figure 6**).

Discussion

The major findings of the present study are that miR-21 is a novel regulator of AS-IV-dependent angiogenesis. We found that AS-IV was able to promote angiogenesis after AMI in rats; furthermore we indicated that miR-21 mimic and AS-IV both have the potential of activating angiogenesis, whereas miR-21 inhibitor blocked the angiogenesis of AS-IV in EA-hy926 cells. We also found that AS-IV could increase the VEGF and AKT expression by regulating miR-21, and these substantial effects were reversed after treatment with the miR-21 inhibitor. Thus, we presented that AS-IV induced angiogenesis was attributed to the activation of VEGF/AKT signaling medicated by miR-21.

MicroRNAs (miRNAs) are short non-coding RNAs that have been identified in a variety of organisms and have been implicated in the control of a wide range of physiological pathways such as development, differentiation, growth and cell metabolism [26-28], particularly in the cardiovascular system [29]. Recent studies suggested that miRNAs contribute to haemodynamically dependent cardiogenesis and angiogenesis [30, 31], and the miR-21 is a expressed during cardiac remodeling and appears to be functional in cardiovascular diseases [32]. In our present research, by using miR-21 mimics and inhibitors, we provided the direct evidences that miR-21 expression was involved in the process of cell proliferation and angiogenesis by AS-IV in vivo and EA-hy926 cells.

AKT (also known as protein kinase B) is a major component in regulating cell proliferation, migration, and survival [33, 34]. Furthermore, a report showed that miR-21 is up-regulated in cardiac fibroblasts in the failing heart, where it represses the expression of Sprouty homolog 1

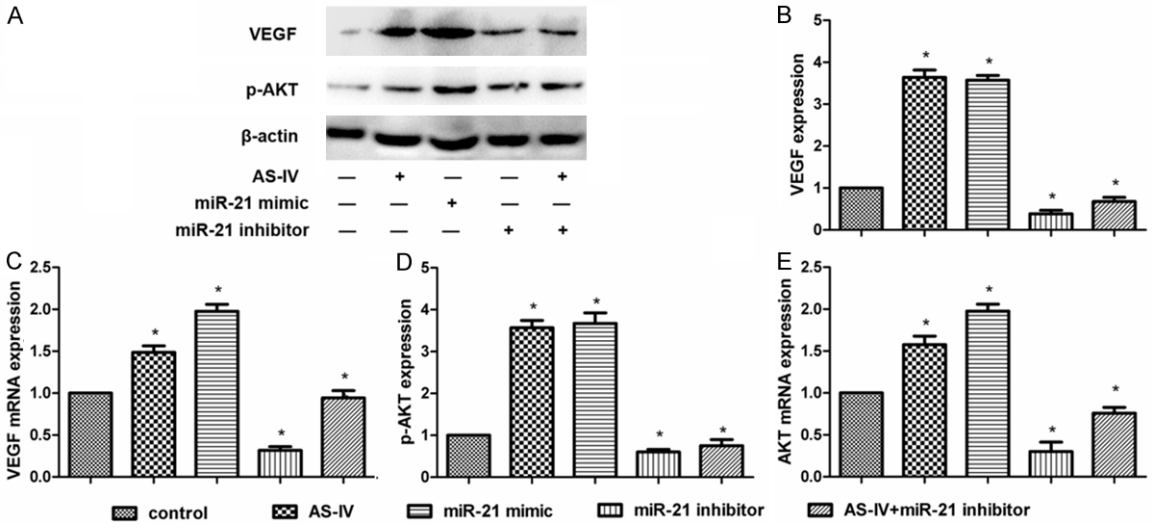

Figure 6. Cells were treated with the miRNA-21 mimics and inhibitors for 48 h, another group with 100 μg/L AS-IV for 24 h. A. Cellularlysate from EA-hy926 cells was used to measure VEGF levels by western blot. B. Bar graph represents VEGF levels in each group. C. Total RNA was extracted and real-time PCR was used to detect the VEGF mRNA levels. D. Bar graph represents p-AKT levels in each group. E. AKT mRNA level was measured by real-time PCR. Data are expressed as the mean ± S.E.M. Data shown are representative of three independent experiments. *: P<0.05 versus control group.

(Spry-1), a negative regulator of the extracellular signal-regulated kinase/mitogen-activated protein (ERK-MAP) kinase [35] AKT and extracellular regulated kinases-1/2 are activated by miR-21. Moreover, an interesting study declared that miR-21 induced angiogenesis through AKT activation and HIF-1α expression, overexpression of miR-21 in DU145 cells increased the expression of HIF-1α and VEGF [36]. Therefore, underlying the results of VEGF, AKT expression enhancement, we demonstrated that miR-21-induced substantial gene alteration was the central mechanism of Astragaloside IV-dependent angiogenesis.

In summary, our present study indicates that AS-IV was a novel regulator of VEGF signaling pathway and angiogenesis through regulating miR-21 in vivo and vitro and administration with AS-IV has notable benefits on rats after AMI. Given our evolving understanding of AS-IV and cardiovascular diseases, AS-IV therapy could be effective in ischemic heart diseases as a novelty approach.

Acknowledgements

This work was supported by grants from National Natural Science Foundation of China (NSFC) 81273943 and 81573908.

Disclosure of conflict of interest

None.

Address correspondence to: Drs. Xiaohu Chen and Jiandong Chen, Department of Cardiology, Jiangsu Province Hospital of Traditional Chinese Medicine, The Affiliated Hospital of Nanjing University of Chinese Medicine, Hanzhong Road 155#, Nanjing 210029, Jiangsu, P. R. China. E-mail: chenxhdoctor@sina.com (XHC); lamala@126.com (JDC)

References

[1] Wang S, Li J, Huang H, Gao W, Zhuang C, Li B, Zhou P and Kong D. Anti-hepatitis B virus activities of astragaloside IV isolated from radix Astragali. Biol Pharm Bull 2009; 32: 132-135.

[2] Zhang N, Wang XH, Mao SL and Zhao F. Astragaloside IV improves metabolic syndrome and endothelium dysfunction in fructose-fed rats. Molecules 2011; 16: 3896-3907.

[3] Oh HA, Choi HJ, Kim NJ and Kim DH. Anti-stress effect of astragaloside IV in immobilized mice. J Ethnopharmacol 2014; 153: 928-932.

[4] Chan WS, Durairajan SS, Lu JH, Wang Y, Xie LX, Kum WF, Koo I, Yung KK and Li M. Neuroprotective effects of Astragaloside IV in 6-hydroxydopamine-treated primary nigral cell culture. Neurochem Int 2009; 55: 414-422.

[5] Miller AL. Botanical influences on cardiovascular disease. Altern Med Rev 1998; 3: 422-431.

[6] Zhao M, Zhao J, He G, Sun X, Huang X and Hao L. Effects of astragaloside IV on action potentials and ionic currents in guinea-pig ventricular myocytes. Biol Pharm Bull 2013; 36: 515-521.
[7] Tu L, Pan CS, Wei XH, Yan L, Liu YY, Fan JY, Mu HN, Li Q, Li L, Zhang Y, He K, Mao XW, Sun K, Wang CS, Yin CC and Han JY. Astragaloside IV protects heart from ischemia and reperfusion injury via energy regulation mechanisms. Microcirculation 2013; 20: 736-747.
[8] He Y, Xi J, Zheng H, Zhang Y, Jin Y and Xu Z. Astragaloside IV inhibits oxidative stress-induced mitochondrial permeability transition pore opening by inactivating GSK-3beta via nitric oxide in H9c2 cardiac cells. Oxid Med Cell Longev 2012; 2012: 935738.
[9] Zhang S, Tang F, Yang Y, Lu M, Luan A, Zhang J, Yang J and Wang H. Astragaloside IV protects against isoproterenol-induced cardiac hypertrophy by regulating NF-kappaB/PGC-1alpha signaling mediated energy biosynthesis. PLoS One 2015; 10: e0118759.
[10] Zhang Y, Zhu H, Huang C, Cui X, Gao Y, Huang Y, Gong W, Zhao Y and Guo S. Astragaloside IV exerts antiviral effects against coxsackievirus B3 by upregulating interferon-gamma. J Cardiovasc Pharmacol 2006; 47: 190-195.
[11] Zhang L, Liu Q, Lu L, Zhao X, Gao X and Wang Y. Astragaloside IV stimulates angiogenesis and increases hypoxia-inducible factor-1alpha accumulation via phosphatidylinositol 3-kinase/Akt pathway. J Pharmacol Exp Ther 2011; 338: 485-491.
[12] Zhang Y, Hu G, Li S, Li ZH, Lam CO, Hong SJ, Kwan YW, Chan SW, Leung GP and Lee SM. Pro-angiogenic activity of astragaloside IV in HUVECs in vitro and zebrafish in vivo. Mol Med Rep 2012; 5: 805-811.
[13] Wang SG, Xu Y, Chen JD, Yang CH and Chen XH. Astragaloside IV stimulates angiogenesis and increases nitric oxide accumulation via JAK2/STAT3 and ERK1/2 pathway. Molecules 2013; 18: 12809-12819.
[14] Wang S, Chen J, Fu Y and Chen X. Promotion of astragaloside IV for EA-hy926 cell proliferation and angiogenic activity via ERK1/2 pathway. J Nanosci Nanotechnol 2015; 15: 4239-4244.
[15] Chen X, Peng LH, Li N, Li QM, Li P, Fung KP, Leung PC and Gao JQ. The healing and anti-scar effects of astragaloside IV on the wound repair in vitro and in vivo. J Ethnopharmacol 2012; 139: 721-727.
[16] Chen X, Peng LH, Shan YH, Li N, Wei W, Yu L, Li QM, Liang WQ and Gao JQ. Astragaloside IV-loaded nanoparticle-enriched hydrogel induces wound healing and anti-scar activity through topical delivery. Int J Pharm 2013; 447: 171-181.
[17] Pepper MS. Manipulating angiogenesis. From basic science to the bedside. Arterioscler Thromb Vasc Biol 1997; 17: 605-619.
[18] Bartel DP. MicroRNAs: genomics, biogenesis, mechanism, and function. Cell 2004; 116: 281-297.
[19] Kumarswamy R, Volkmann I and Thum T. Regulation and function of miRNA-21 in health and disease. RNA Biol 2011; 8: 706-713.
[20] Thum T, Catalucci D and Bauersachs J. MicroRNAs: novel regulators in cardiac development and disease. Cardiovasc Res 2008; 79: 562-570.
[21] Bauersachs J. Regulation of myocardial fibrosis by MicroRNAs. J Cardiovasc Pharmacol 2010; 56: 454-459.
[22] van Rooij E, Sutherland LB, Liu N, Williams AH, McAnally J, Gerard RD, Richardson JA and Olson EN. A signature pattern of stress-responsive microRNAs that can evoke cardiac hypertrophy and heart failure. Proc Natl Acad Sci U S A 2006; 103: 18255-18260.
[23] Tatsuguchi M, Seok HY, Callis TE, Thomson JM, Chen JF, Newman M, Rojas M, Hammond SM and Wang DZ. Expression of microRNAs is dynamically regulated during cardiomyocyte hypertrophy. J Mol Cell Cardiol 2007; 42: 1137-1141.
[24] Kolpa HJ, Peal DS, Lynch SN, Giokas AC, Ghatak S, Misra S, Norris RA, Macrae CA, Markwald RR, Ellinor P, Bischoff J and Milan DJ. miR-21 represses Pdcd4 during cardiac valvulogenesis. Development 2013; 140: 2172-2180.
[25] Fleissner F, Jazbutyte V, Fiedler J, Gupta SK, Yin X, Xu Q, Galuppo P, Kneitz S, Mayr M, Ertl G, Bauersachs J and Thum T. Short communication: asymmetric dimethylarginine impairs angiogenic progenitor cell function in patients with coronary artery disease through a microRNA-21-dependent mechanism. Circ Res 2010; 107: 138-143.
[26] Ambros V. MicroRNA pathways in flies and worms: growth, death, fat, stress, and timing. Cell 2003; 113: 673-676.
[27] Krutzfeldt J, Rajewsky N, Braich R, Rajeev KG, Tuschl T, Manoharan M and Stoffel M. Silencing of microRNAs in vivo with 'antagomirs'. Nature 2005; 438: 685-689.
[28] Jonas S and Izaurralde E. Towards a molecular understanding of microRNA-mediated gene silencing. Nat Rev Genet 2015; 16: 421-433.
[29] Small EM and Olson EN. Pervasive roles of microRNAs in cardiovascular biology. Nature 2011; 469: 336-342.
[30] Miyasaka KY, Kida YS, Banjo T, Ueki Y, Nagayama K, Matsumoto T, Sato M and Ogura T. Heartbeat regulates cardiogenesis by sup-

pressing retinoic acid signaling via expression of miR-143. Mech Dev 2011; 128: 18-28.
[31] Nicoli S, Standley C, Walker P, Hurlstone A, Fogarty KE and Lawson ND. MicroRNA-mediated integration of haemodynamics and Vegf signalling during angiogenesis. Nature 2010; 464: 1196-1200.
[32] Cheng Y and Zhang C. MicroRNA-21 in cardiovascular disease. J Cardiovasc Transl Res 2010; 3: 251-255.
[33] Scheid MP and Woodgett JR. PKB/AKT: functional insights from genetic models. Nat Rev Mol Cell Biol 2001; 2: 760-768.
[34] Franke TF. PI3K/Akt: getting it right matters. Oncogene 2008; 27: 6473-6488.
[35] Thum T, Gross C, Fiedler J, Fischer T, Kissler S, Bussen M, Galuppo P, Just S, Rottbauer W, Frantz S, Castoldi M, Soutschek J, Koteliansky V, Rosenwald A, Basson MA, Licht JD, Pena JT, Rouhanifard SH, Muckenthaler MU, Tuschl T, Martin GR, Bauersachs J and Engelhardt S. MicroRNA-21 contributes to myocardial disease by stimulating MAP kinase signalling in fibroblasts. Nature 2008; 456: 980-984.
[36] Liu LZ, Li C, Chen Q, Jing Y, Carpenter R, Jiang Y, Kung HF, Lai L and Jiang BH. MiR-21 induced angiogenesis through AKT and ERK activation and HIF-1alpha expression. PLoS One 2011; 6: e19139.